ICANS–XIII
13th Meeting of the International Collaboration on
Advanced Neutron Sources
October 11–14, 1995
Paul–Scherrer–Institut, 5232 Villigen PSI, Switzerland

ON PROTON PULSE LENGTHS AND REP RATES WITH EMPHASIS ON SANS

Harald Conrad

Institut für Festkörperforschung
Forschungszentrum Jülich
Postfach 1913, D–52425 Jülich, Germany

ABSTRACT

The consequences of different proton pulse characteristics on the performance of neutron scattering instruments are discussed in general for a cryogenic moderator. The possible gain of pulsed operation for both time–of–flight and continuous source applications is outlined. Small angle neutron scattering (SANS), a classical technique at a continuous source is taken as an example to show pros and cons of different source concepts. It is shown that a single number (gain factor) is not sufficient to qualify SANS at a pulsed source. In addition to this integral quantity, a differential gain is defined. The latter can be used to better assess the most adequate source parameter specification.

1. Introduction

All existing spallation neutron sources are pulsed (the SINQ under construction at PSI becoming an exceptional case). This is equivalent to saying that the proton pulse duration t_p is negligibly short compared to both the slowing down times to thermal equilibrium in any moderator, t_e, and the storage times of thermalized neutrons in the moderators, τ. Although both times determine the detailed shape of the neutron pulse for neutrons in thermal equilibrium, the storage time usually dominates. Therefore the latter is responsible for the more or less slowly decaying pulse tails. It is this storage time, which can be changed drastically by moderator "tailoring" (poisoning, decoupling). Shortening the neutron pulse duration this way is essential for improving spectrometer or diffractometer resolution. On the other hand, the average neutron flux of pulsed

Keywords: Long pulse source, high intensity moderator, SANS, differential gain

sources strongly depend on this tailoring. It should be mentioned in this context that tailoring with long pulse sources (several hundred μs to a few ms) does not make sense, as will be discussed below. Although it is not the topic of this paper, we should not forget to mention the well–known fact that only pulsed sources gain two to three orders of magnitude in utilizing epithermal (slowing down) neutrons.

Until recently the only project, which abandoned the concept of a pulsed source in the sense defined at the beginning, was the German 5.5 MW SNQ. There were very good reasons for considering what was called an intensity modulated neutron source (IMNS), i.e. a linac only design with a proton pulse duration (in the final proposal) of 250 μs. Although a pulse compressor was considered as an add–on option, it was not included in the project proper because of the very ambitious source parameters, especially the 2.7×10^{14} protons per pulse at 1.1 GeV to be stored in a single ring. Even more than 10 years later the 5 MW ESS project resorts to two compressor rings, each to carry 2.3×10^{14} ppp at 1.33 GeV. (ESS is planned to operate at 50 Hz instead of 100 Hz with SNQ.)

Probably the most important reason for advocating an IMNS was that except for not utilizing epithermal neutrons most effectively, the performance of virtually all neutron scattering instruments was expected to be superior to equivalent ones at the ILL reactor [R.Scherm and H.Stiller].

As may be already inferred from the discussion above, moderator tailoring does not make sense at an IMNS, because it would only reduce the average neutron flux. The neutron pulse width would still be dominated by the proton pulse duration, as is shown in the next chapter. In the discussion of the pros and cons of source concepts with different proton pulse durations and repetition rates we will not consider moderator tailoring even for pulsed sources, for it would adulterate a fair comparison. In such a comparison we have at least to keep the moderator parameters fixed when varying the proton pulse data.

2. Pulse shapes, peak fluxes and rep rates

In the following we will consider only a cryogenic moderator in its so–called high intensity configuration, i.e. there are neither neutron poisons within nor decouplers around the moderator. To be quantitative we will rely on experimental data obtained with a liquid hydrogen moderator embedded in various reflector materials [G.Bauer et al. 1985]. The results are reproduced in Table 1.

Table 1 Storage times τ, average neutron fluxes $<\phi>$ and cold neutron pulse widths for a liquid H_2 moderator. ^{238}U target. The neutron pulse widths are calculated assuming a proton pulse duration $t_p = 250\ \mu s$. After G.S.Bauer et al. 1985.

reflector	neutron storage time $\tau/\mu s$	average flux $<\phi>/10^{14}cm^{-2}s^{-1}$	cold neutron pulse width FWHM/μs
Pb	230	4.3	320
C	350	5.4	390
D_2O	710	6.6	620

In order to be specific, we have selected the carbon reflected case from Table 1. Using the storage time $\tau = 350\ \mu s$, the neutron pulse shapes depicted in Figure 1 are calculated according to the relations

$$\begin{aligned} \phi(t) &= \phi_\infty \cdot (1 - e^{-t/\tau}) && t < t_p \\ \hat{\phi} &= \phi(t = t_p) = \phi_\infty \cdot (1 - e^{-t_p/\tau}) && \text{peak flux} \\ \phi(t) &= \hat{\phi} \cdot e^{-(t - t_p)/\tau} && t > t_p \end{aligned} \qquad (1)$$

where $\phi_\infty = <\phi> \cdot \frac{t_{rep}}{t_p}$ is the asymptotic flux, which would be obtained with d.c. proton peak current. Obviously, this asymptotic flux is related to the time average flux $<\phi>$ of a pulsed or modulated source by the last relation above, where t_{rep} is the time between two source pulses. These relations do not contain the slowing down time t_e, but are nevertheless good approximations, because $\tau >> t_e$ in all cases (see also section 3.1).
Figure 1 depicts the cold moderator response, i.e. the neutron pulse shapes, to several widely differing primary proton pulse shapes. Shown are a comparison of a pulsed source (the ESS concept) to three different long pulse source concepts:

- ESS (5 MW, 1.334 GeV, 50 Hz),
- the former German SNQ (5.5 MW, 1.1 GeV, 100 Hz),
- a linac only variant of the ESS based on the unchopped linac current and the proton pulse length matched in order to roughly equal the SNQ power, and
- a very long pulse source concept with alternating pulse lengths [Mezei, 1993].

Mezei's concept of very long pulses is an attempt to optimize the source utilization. The alternating pulse lengths with half the beam power in 4–ms–pulses at 12.5 Hz are meant to offer low resolution applications like SANS the possibility to exploit a wide

wavelength band (by suppressing the three intermittent pulses), while others use all pulses at 50 Hz. The gain for SANS with this concept will be discussed in more detail in chapter 4.

The neutron pulses plotted in Fig. 1, denoted as time–dependent fluxes, are normalized to the corresponding average neutron fluxes. As the proton beam power in all four cases is about the same, we may directly take the relative heights and shapes of the pulses as a

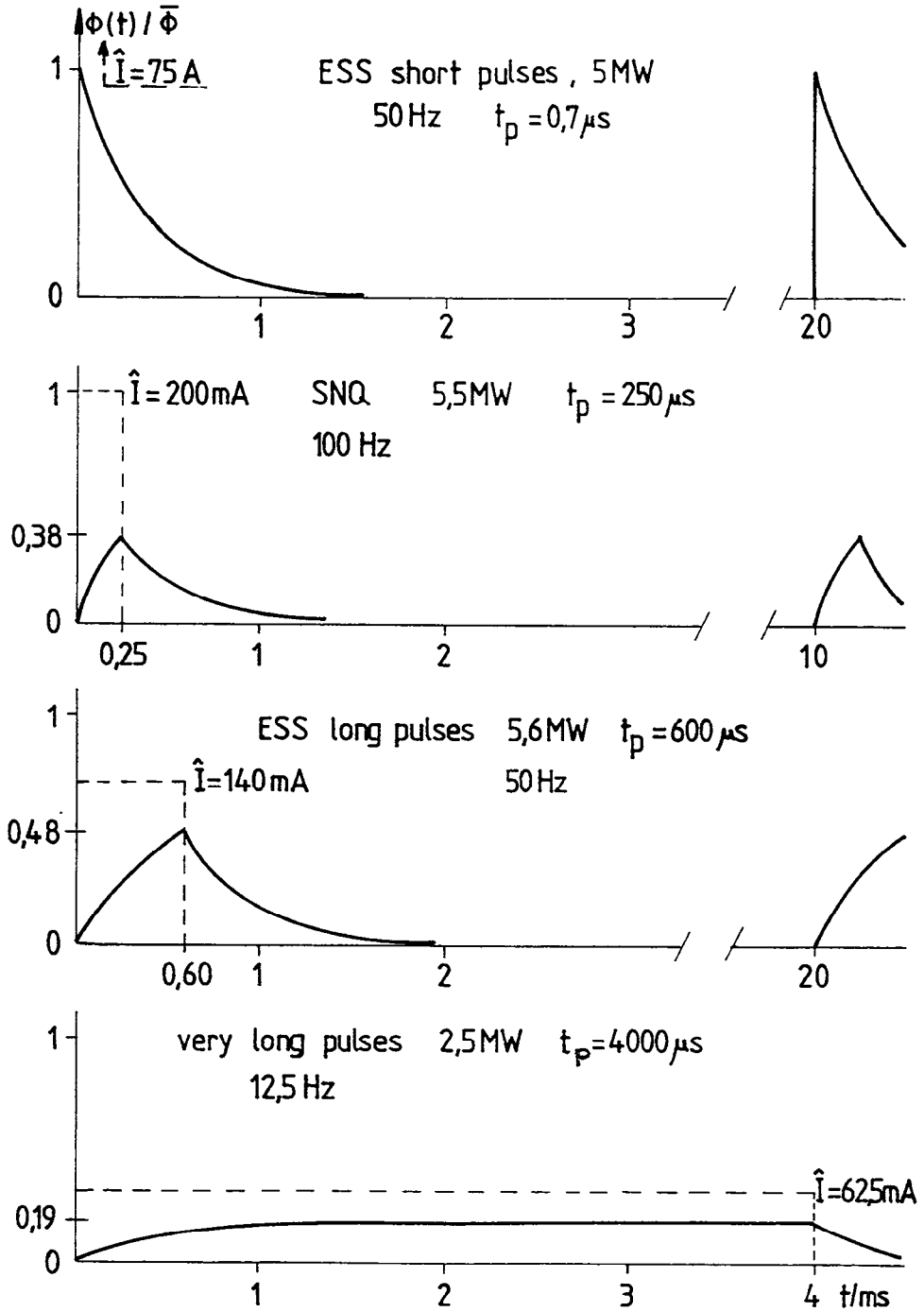

Figure 1 Cold neutron pulse shapes from a coupled, unpoisoned liquid hydrogen moderator surrounded by a graphite reflector for four source concepts: one short pulse and three different long pulse sources. The neutron storage time in this case is $\tau = 350$ μs.

measure of the target–moderator performance. The most striking feature in comparing the four frames in Figure 1 is the (well–known) fact that we only gain about a factor of two in neutron peak flux in compressing e.g. the unchopped ESS limac current by nearly three orders of magnitude. This can easily be verified by calculating the peak flux of equation (1) for infinitely short proton pulse duration t_p

$$\lim \hat{\phi} = \frac{t_{rep.}}{\tau} \cdot \langle\phi\rangle$$

and comparing this to the peak flux for e.g. $t_p = 2\tau$

$$\hat{\phi}(t_p = 2\tau) \simeq 0.43 \cdot \frac{t_{rep.}}{\tau} \cdot \langle\phi\rangle.$$

It is evident now from Figure 1 that the neutron pulse widths do not essentially depend on the proton pulse width as stated in the Introduction.

3. General gain considerations

There are mainly two reasons why we expect a gain in counting rate of useful neutrons at an instrument's detector with a pulsed or intensity modulated source. Firstly, the peak flux of even a low power source may exceed the average flux of a high flux reactor and, secondly, we can attempt to utilize a polychromatic neutron band during times between the pulses. It is not an easy task to quantify a gain for a particular instrument. This is due to the fact that the instrument suites at reactors and the existing pulsed sources have been devised under strongly differing prerequisites. We do not have many examples if any at all, where a reliable comparison was made of the performance of a particular instrument at both a reactor and a pulsed source. A case, which is certainly close to this requirement, is the work of Schäfer et al. They tested a diffractometer set–up including identical primary collimation, an identical sample and an identical position sensitive detector both at ISIS and the FRJ–2 reactor [Schäfer et al. 1992]. Unfortunately, this comparison cannot simply be quantified by a single gain factor, because the number of measured Bragg reflections differ in the two cases. This situation we will often encounter.

3.1 Gain for time–of–flight applications

In contrast to the just mentioned case we may well be able to find in a straightforward manner gain factors for direct geometry time–of–flight instruments. Consider a chopper spectrometer with chopper frequency f_{ch} and imagine the same instrument operating at a pulsed source whose rep rate is f_{rep}. Then the obvious gain factor G is defined by

$$G = \frac{f_{rep} \cdot \hat{\phi}}{f_{ch} \cdot \phi_r} = \frac{1 - e^{-t_p/\tau}}{f_{ch} \cdot t_p} \cdot \frac{\langle\phi\rangle}{\phi_r} \qquad (3)$$

where we have used equ. 1. ϕ_r denotes the (constant) reactor neutron flux. The gain appears to be independent of the rep rate of the pulsed (or intensity modulated) source. In order to understand this it is instructive to distinguisch two cases.

– Comparison short pulse source/reactor

Letting t_p tend to zero we get

$$G = \frac{1}{\tau \cdot f_{ch}} \cdot \frac{<\phi>}{\phi_r} \qquad (4)$$

In this case, the gain is essentially independent of the source rep rate when keeping the average flux fixed. In other words, halving the rep rate requires doubling the number of protons per pulse for fixed pulse duration! It may be worthwhile to point out in this context that reducing the proton pulse duration below the slowing down time t_e does not raise the peak flux anymore. As an approximation we may replace equ. 4 by equ. 3 with inserting t_e for t_p. Taking $t_e = 20\mu s$ we get a result, which is lower by less than 3% than that using equ. 4.
The crucial factor $1/(\tau f_{ch})$ in equ. 4, which gives the gain with a pulsed source compared to a reactor of equal flux, is for cold neutrons of the order of

$$\frac{1}{\tau \cdot f_{ch}} = \frac{1}{3.5 \times 10^{-4} \times 200} \simeq 14$$

– Comparison long pulse source/reactor

Here the situation is a bit more involved, if we accept that the duty cycle $d = t_p/t_{rep}$ of a linac is not an entirely free parameter [G.Bauer, 1995]. If we assume a fixed duty cycle (the linac peak current cannot easily be increased), the gain actually increases with increasing rep rate $f_{rep} = 1/t_{rep}$. This is evident from rewriting equ. 3 in the form

$$G = G(f_{rep}) = \frac{f_{rep} \cdot [1 - e^{-c/(\tau f_{rep})}]}{c \cdot f_{ch}} \cdot \frac{<\phi>}{\phi_r}.$$

The graph of this function is shown in Figure 2. It should be mentioned that the gain plotted in Figure 2 approaches the short pulse case for very high rep rates. Clearly, this limiting case will not be reached, because it would not make sense to operate the pulsed source at rep rates higher than any reasonable chopper frequency of a reactor instrument.
Physically, the rep rate dependent gain can be understood by the non–linearity of the rising part of the neutron pulse as depicted in Figure 3. Doubling the peak current during t_p would double the peak flux, but doubling t_p at fixed peak current would not!

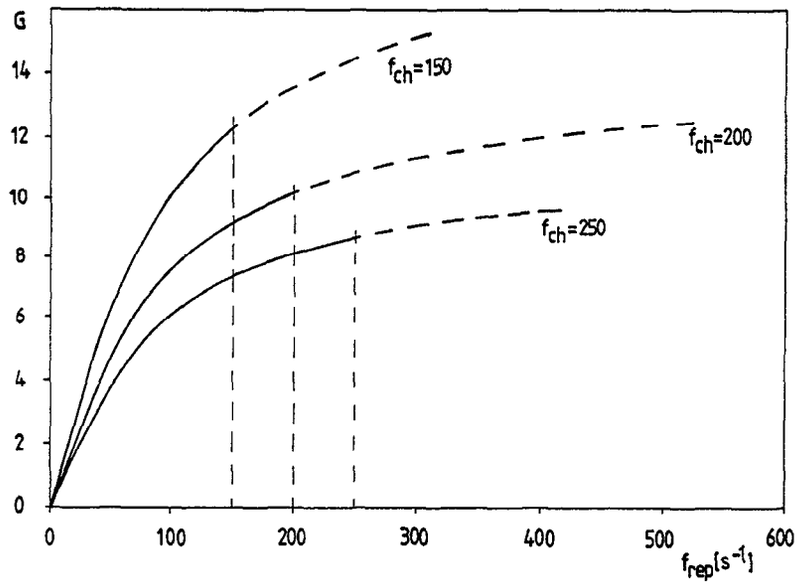

Figure 2 Rep rate dependent gain factor for a long pulse source with fixed duty cycle c = 0.05.

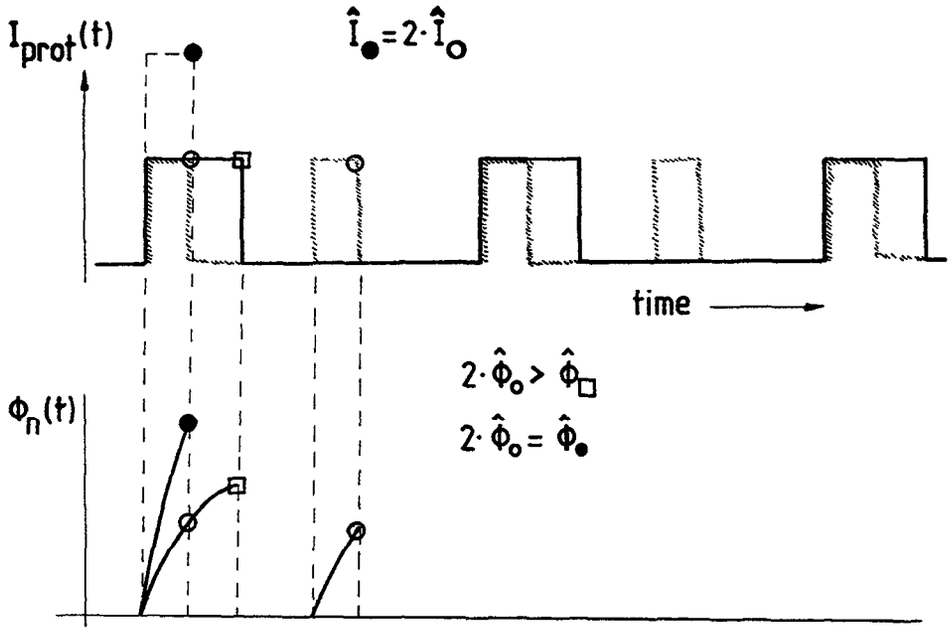

Figure 3 Increasing the rep rate at fixed duty cycle enhances the gain for a long pulse source as long as $f_{rep} \leq f_{ch}$

3.2 Gain for wide wavelength band applications

We are now turning to discuss the possibility of exploiting the time interval between pulses, i.e. the utilization of different wavelengths sequentially in time. In order to obtain as wide a wavelength band $\Delta\lambda$ as possible we demand short source–detector distances L and/or low rep rates. This can readily be seen from the familiar distance–time diagram shown in Figure 4, or from the well–known relation

$$\Delta\lambda = \frac{\text{const}}{L \cdot f_{rep}}, \qquad (\text{const} = 3956 \text{ Åms}^{-1}). \qquad (5)$$

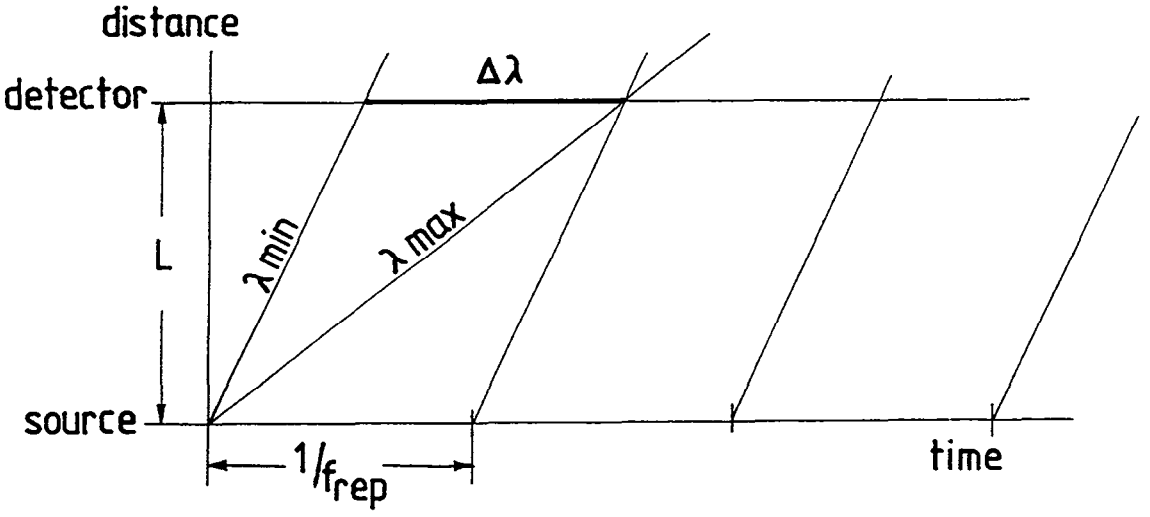

Figure 4 Distance—time—diagram for determining the maximum wavelength band

If L is determined by constraints like source shielding, minimum sample–detector distances or others, we might request the source with the lowest possible rep rate. This is now a conflicting situation, for we just showed that long pulse source (direct geometry) t–o–f applications demand high rep rates. In the case of short pulse sources the number of protons per pulse sets a technical lower limit to the rep rate at a given average beam power. In the remaining part of this paper we will discuss the consequences of different pulse lengths and rep rates on the possible gain for small angle neutron scattering.

4. Gain considerations for small angle neutron scattering

4.1 The influence of resolution requirements

We just stated that we want to use the highest feasible wavelength band. But we have to look somewhat closer to that demand, when we talk about applying this rule to SANS. We have to take into account the required resolution R, which can be written in different ways and is typically of the order of 0.1 to 0.15

$$R = \frac{\delta\lambda}{\lambda} = \frac{\delta t}{t} = \frac{\delta t}{L/v} \stackrel{!}{=} 0.1$$

where δt cannot be lower than the source neutron pulse width, which is roughly given by the moderator storage time τ (compare Fig. 1). This lower limit sets in turn a lower limit on the useful wavelength

$$\lambda_{min} = \frac{const}{L \cdot R} \cdot \delta t.$$

Setting $\delta t \simeq \tau \simeq 5 \times 10^{-4}$s, we can calculate the cut–off wavelength λ_{min} for the three main source types presented in Figure 1.

– short pulse source: $\lambda_{min} \simeq 20/L$

Inserting L in meters we see that there is virtually no restriction, because even a very short instrument with L = 10 m (note: 6 m shielding thickness) would not pose a serious limit on λ (see Figure 5 below).

– long pulse source: $\lambda_{min} \simeq 20/L$,

which is the same as with the short pulse source, as long as we stick to the rule that the proton pulse length should be matched to the storage time, $t_p \simeq \tau$ (SNQ: $t_p = 250\ \mu s$).

– "very" long pulse source: $\lambda_{min} = 160/L$,

if we choose e.g. $t_p = 4000\ \mu s$. Even a 40–m–machine already has a cut–off at 4 Å.

Let us now turn to quantify the gain we can expect from exploiting a wide band of wavelengths. There will be mainly two points of view. An obvious definition of a gain is the ratio of the total detector counts from both the pulsed and the continuous operation. This is a common procedure and we will call this the integral gain. It certainly gives an idea of the advantage of the method, but the information content of a measurement is not only contained in the integral detector counts. The momentum transfer dependence of the scattered intensity I(Q) is the crucial point, so we will define a Q–dependent gain, which we call the differential gain. With the latter we have furthermore to distinguish between cases with and without restrictions on the useful band. In this context it may be useful to remark that the resolution imposed cut–off is equvalent to one, which we had to impose, if we had to avoid double Bragg scattering, i.e. $\lambda > \lambda_{bragg}$.

4.2 Integral gain

In calculating the ratio just mentioned we have to bear in mind that the total intensity scattered into forward direction is proportional to λ^2 [Guinier]. Therefore we will use the modified flux (better: current) $\lambda^2 \cdot j(\lambda)$ in computing the gain. Furthermore we will always assume that the experiment at the continuous source will be performed using the optimum wavelength λ_0, i.e. at the maximum in the $\lambda^2 \cdot j(\lambda)$–curve. So we define the integral gain as

$$G = \frac{\int_{\Delta\lambda} \lambda^2 j(\lambda) d\lambda}{\lambda_0^2 \cdot j(\lambda_0)\delta\lambda} \qquad (6)$$

$\delta\lambda$ is taken as the FWHM of a typical triangular resolution element with $\delta\lambda/\lambda = 0.1$. In order to get the most from this integral, $\Delta\lambda$ has to be positioned such over the spectrum that $\lambda^2_{1o} j(\lambda_{1o}) = (\lambda_{1o} + \Delta\lambda)^2 j(\lambda_{1o}+\Delta\lambda)$, as indicated in Figure 5. Also shown in Figure 5 is the shift of $\Delta\lambda$ to longer wavelengths, if we cannot utilize neutrons below λ_{min}. Data collection at the pulsed source would be performed by non–equidistantly time slicing the interval $\Delta\lambda$ (resp. Δt) in order to keep the resolution fixed for every $\delta\lambda$–(δt)–bin (compare Fig. 5).

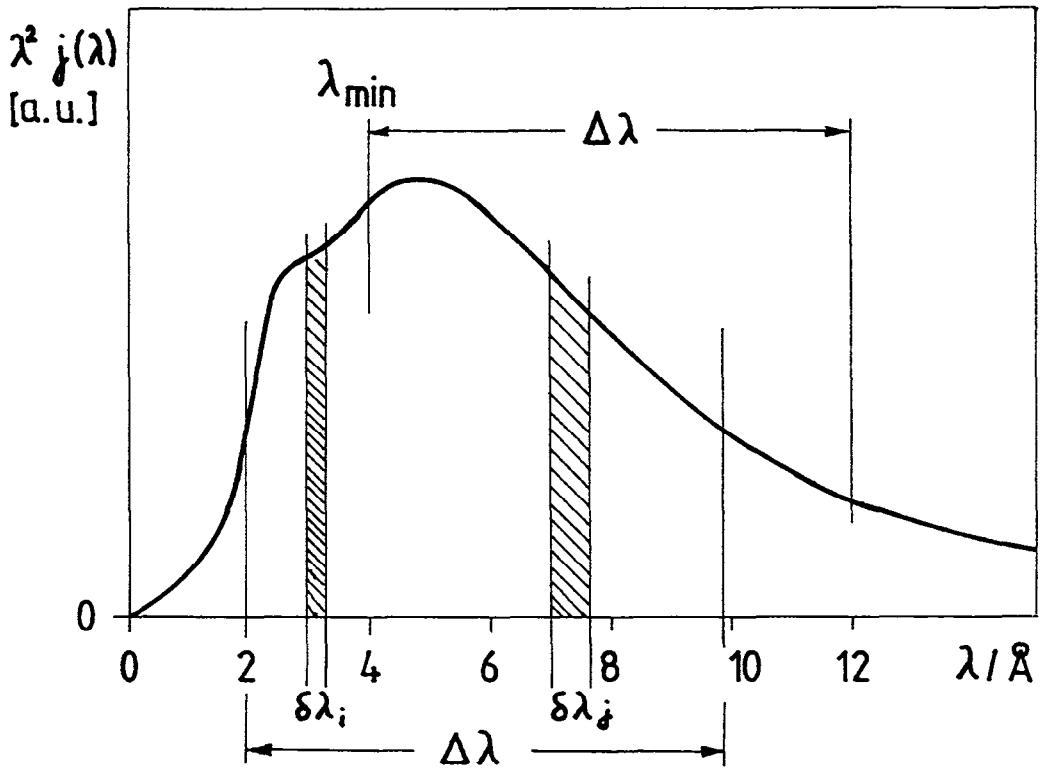

Figure 5 Positioning $\Delta\lambda(L,f_{rep})$ over the modified cold spectrum $\lambda^2 j(\lambda)$, where $j(\lambda)$ is the experimental ISIS 25 K moderator data.

In Figure 6 are compiled graphically all the gain factors calculated according to equ. 6 together with equ. 5. The scale is normalized to the average cold neutron flux of a 5 MW spallation source with a liquid hydrogen moderator (G = 1).

Two features of these integral gain factor functions should be pointed out. Firstly as expected, the wider $\Delta\lambda$ by suppressing 4 in 5 pulses (the 1 MW ESS target station L) cannot compensate the 80% loss in average neutron flux. The corresponding differential gain will be discussed in the following section. Secondly, the very long pulse source

variant at half the proton beam power of ESS would be superior to the latter for instruments longer than 30 m. Although the shock–like load of the target is absent with these long pulses, the 2.5 times larger temperature jump per pulse may pose a serious fatigue problem. This has to be investigated thoroughly.
We should not forget to mention the strong decrease of the long pulse gain factors for short distances, which is due to the resolution requirements and the corressponding shift of the $\Delta\lambda$–band to longer wavelengths (see section 4.1).
Finally we would like to point out that we cannot simply scale the short pulse 1 MW ESS case in order to outperform the 2.5 MW long pulse versions, because the enhanced shock load could not be taken by the target. Furthermore, the number of compressor rings had to altered from 2 to 6, a very unrealistic scenario.

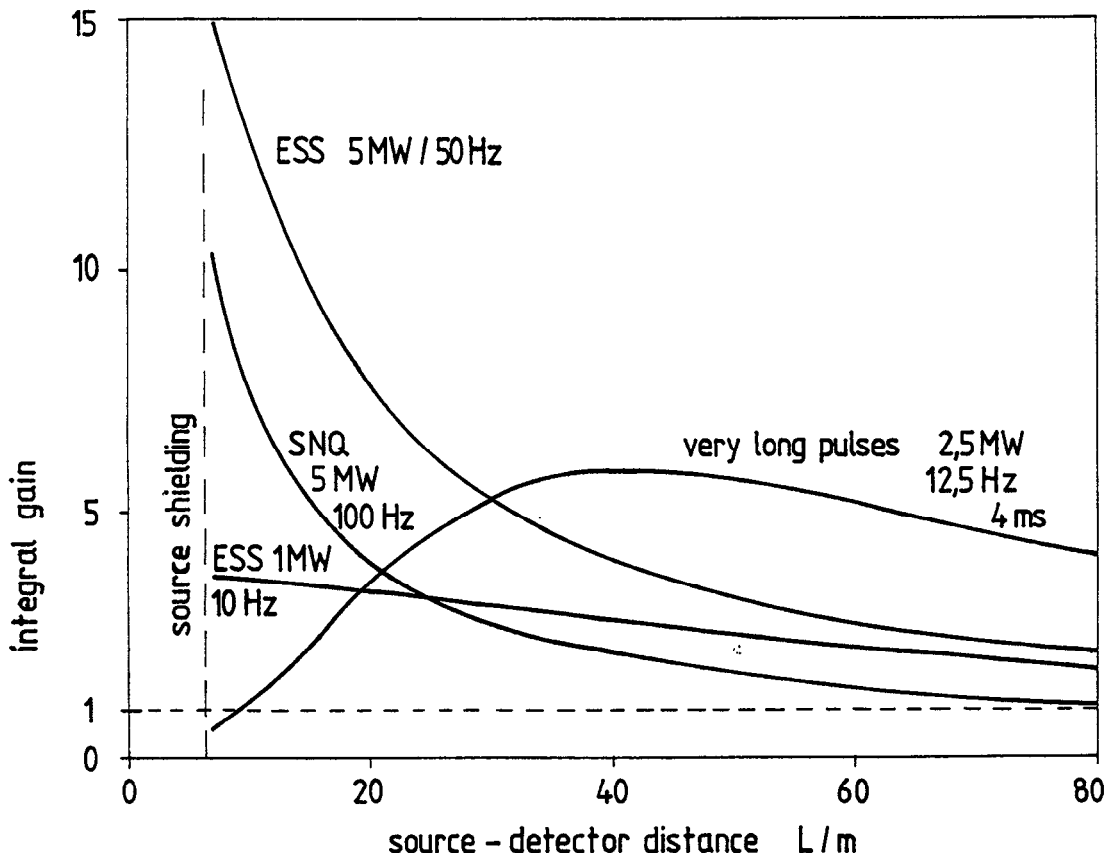

Figure 6 Integral gains for SANS as a function of source to detector distance for various source concepts. (G = 1 represents the continuous operation of a 5 MW source or the corresponding reactor equivalent.)

4.3 Differential gain G(Q)

Let us consider the standard SANS instrument equipped with a 2–dimensional position sensitive detector. At a continuous source we would select the optimum wavelength λ_0 from the moderator spectrum and accumulate the scattered intensity I(Q) from the

sample as a function of the momentum transfer Q. The latter is a single–valued function of the detector element coordinates x and y, say. At a pulsed source the Q–value corresponding to a certain (x,y) changes when scanning the $\Delta\lambda$–band. In other words, many detector elements represent as a function of time (wavelength) a certain Q–value. The differential gain, which we may also call a Q–dependent gain G(Q), therefore is obtained by summing up all the scattered intensities from different detector elements corresponding to a fixed Q–value. Clearly, the detector response depends on the actual sample, but for a quantification of G(Q) we may as well imagine a perfectly incoherent scatterer. On this basis we can easily depict G(Q), which has been calculated in the following according to the expression

$$G(Q) = \frac{\sum_{t\text{-bins}} I_t(Q)}{I_{mono}(Q)}.$$

The t–bins (λ–bins) are time (wavelength) slices of the spectrum of Fig. 5 with constant $\delta\lambda_n/\lambda_n$. The intensity in each slice t_n being scattered incoherently gives rise to a constant detector response $I_t(Q)$ between $Q_{min}(t_n)$ and $Q_{max}(t_n)$, with $Q_{max}(t_n)/Q_{min}(t_n)$ set equal to 8 (corresponding to detector pixel ratios x_{max}/x_{min} or $y_{max}/y_{min} = 8$), independent of t_n.

Examples

In the following we will show the results of these calculations for two instrument configurations and three different rep rate/pulse length combinations. We denote the moderator detector distance by L, moderator sample distance by D and sample detector distance by d, i.e. L = D + d.

- L = 15 m: D = 10 m, d = 5 m. ($1\ \mu s \leq t_p \leq 500\ \mu s$)

In Fig. 7a is shown the differential gain G(Q) for a short pulse or long ($t_p \leq \tau$) pulse source operated at 50 Hz. In the adjacent Fig. 7b is shown the gain when operating the source at reduced rep rate and power (10 Hz, one pulse in five). The horizontal rectangles on the abszissa depict the corresponding detector response with a continuous source of equal average flux as the 50 Hz pulsed source. Clearly, the accessible Q–range in one detector setting has doubled in the 10 Hz case, but only at very low intensity level. The discontinuous contour of the gain functions reflect the time slicing of the primary spectrum.

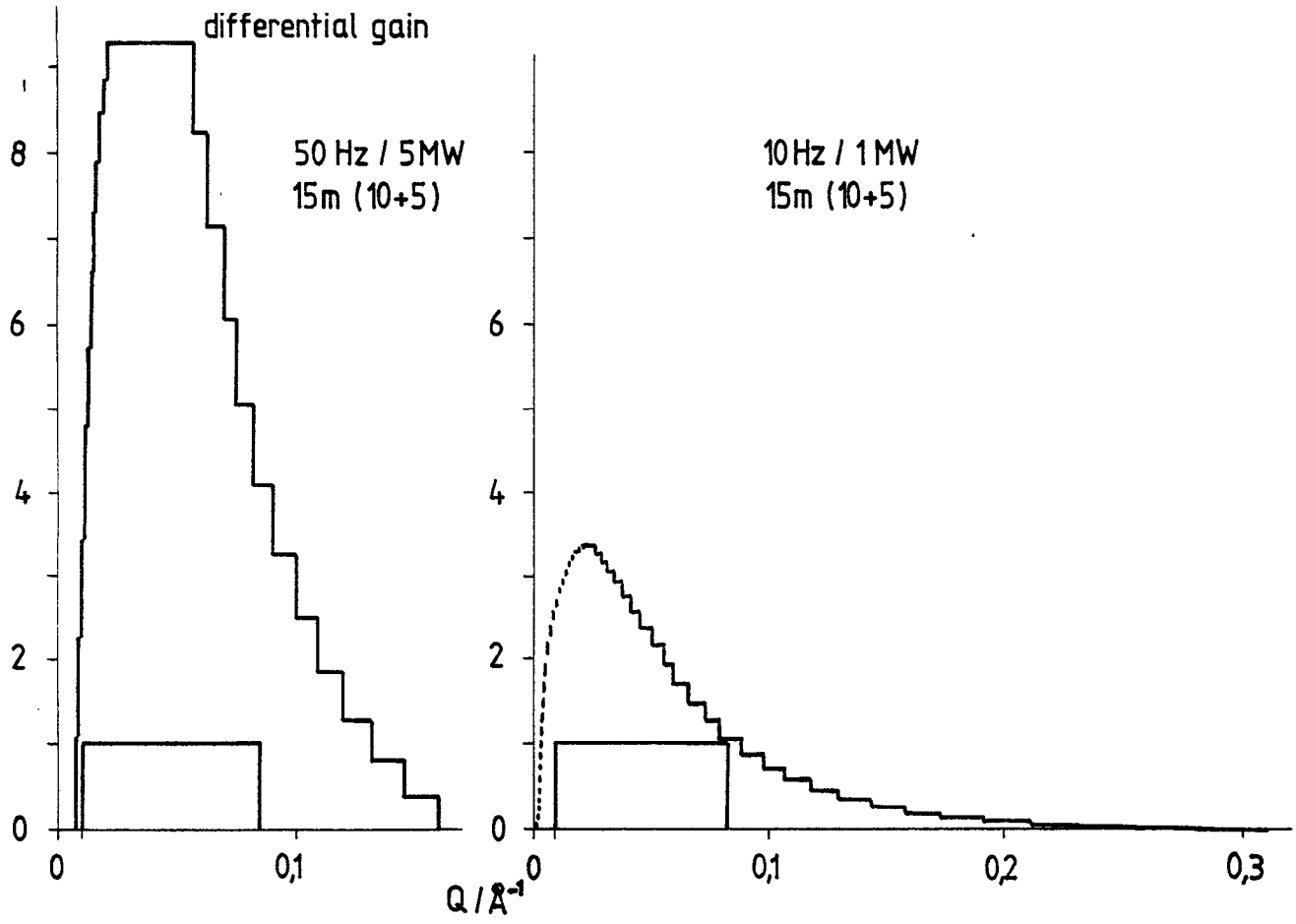

Figure 7 a: Differential gain G(Q) for pulsed or intensity modulated operation at 50 Hz (e.g. 5 MW) and detector setting L = D + d = 10 + 5 m. b: G(Q) at 10 Hz (i.e. 1 MW).

- L = 40 m: D = 20 m, d = 20 m. $(1\ \mu s \leq t_p \leq 500\ \mu s)$

In Fig. 8a is shown the differential gain G(Q) for a short pulse or long ($t_p \leq \tau$) pulse source again operated at 50 Hz. In Fig. 8b is shown the gain when operating the source at reduced rep rate and power (10 Hz, one pulse in five). The horizontal rectangles on the abszissa indicate as in Fig. 7 the detector response with a continuous source of equal average flux. The absolute scale of these graphs is of course different from those in Fig. 7. The differential gain is calculated within a chosen detector setting only. No attempt has been made to include an additional gain due to the fact that different detector settings in the continuous case may be comprised in one setting in the pulsed case because of the wider Q–range (compare Fig. 7).

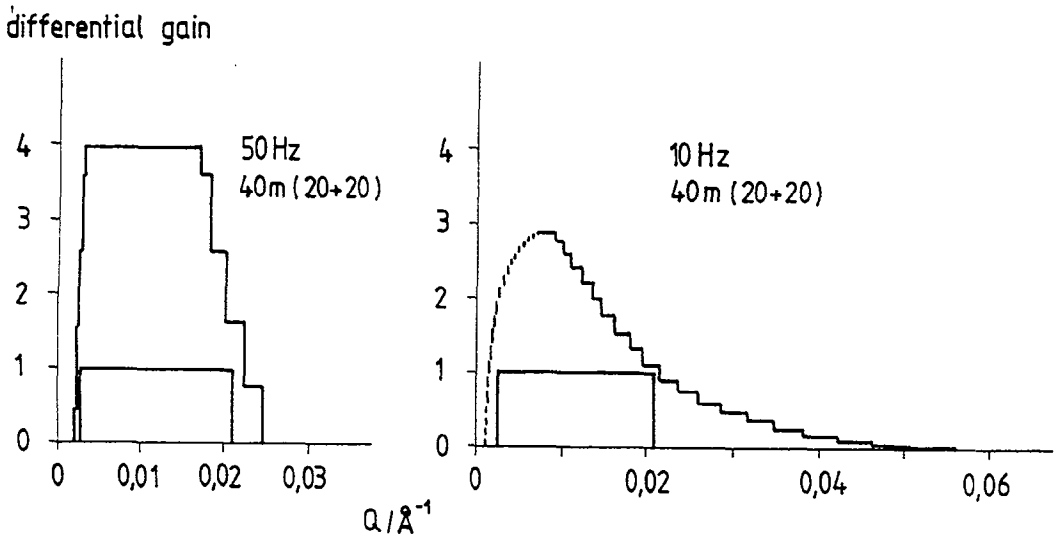

Figure 8 a: Differential gain G(Q) for pulsed or intensity modulated operation at 50 Hz (e.g. 5 MW) and detector setting L = D + d = 20 + 20 m. b: G(Q) at 10 Hz (i.e. 1 MW).

- L = 40 m: D = 20 m, d = 20 m. ($t_p = 4000\ \mu s$)

For the 40–m–setting we have as well calculated the differential gain for a source with very long pulses, i.e. 4 milliseconds. The source is imagined to operate at 12.5 Hz at an average power of 2.5 MW. The result shown in Fig. 9 is correctly scaled and can be directly compared to Fig. 8. Because of the limitation of the $\Delta\lambda$–band to wavelengths larger than 4 Å (due to the long pulses) the accessible Q–range is strongly reduced as compared to the 1 MW/10 Hz case.

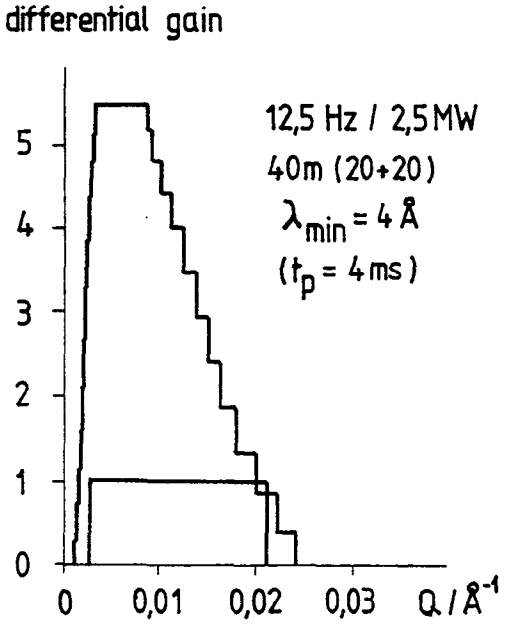

Figure 9 Differential gain G(Q) for a very long pulse source.

5. Conclusions

1. Short proton pulses are not necessary for applications, where a coarse primary wavelength resolution is needed only, such as small angle neutron scattering, neutron spin echo spectroscopy, diffuse scattering or others. On the other hand, they do not harm the performance of these instruments, if

- one can produce them at all (i.e. $\simeq 5\times 10^{14}$ protons per pulse with $t_p \leq 1$ μs, ESS)
- one can afford the investment (compressors or synchrotrons)
- the target can stand the stress loads.

2. If one or several of the following reasons are true,

- a linac of sufficient power exists,
- one is aiming at an improved reactor performance "only", (intensity modulated source)
- one is planning for a spallation source with more than one target station,
- a high power ($\geq$ 5 MW) short pulse project should be realized in stages (e.g. in bypassing the ring(s) in a linac/compressor version),

then long proton pulses matched to the neutron storage time τ are recommended at a rep rate not too far below typical cold neutron chopper frequencies, i.e.

$t_p \simeq 0.3 \ldots 0.6$ ms

$f_{rep} \simeq 50$ Hz.

3. There is no "right" solution: t_p and f_{rep} have to be a compromise.

4. The usefulness of very long proton pulses ($t_p >> \tau$) is not convincing, particularly in view of target problems with thermal cycling.

6. References

G.S.Bauer, H.Conrad, W.Fischer, K.Grünhagen and H.Spitzer; Proc. ICANS–VIII (1985), RAL–85–110

G.S.Bauer, Workshop on Neutron Instrumentation for a Long Pulse Spallation Source, Berkeley (1995)

A.Guinier and G.Fournet, Small Angle Scattering of X–Rays (1955)

F.Mezei, ICANS–XII, Vol.I, 377 (1993)

W.Schäfer, E.Jansen, R.Skowronek, G.Will. K.S.Knight and J.L.Finney; Nucl. Instr. and Meth. A317 (1992) 202

R.Scherm and H.Stiller (eds.), Proceedings of the Workshop on Neutron Scattering Instrumentation for SNQ. Jül–Conf–1954 (1994)